

Title	The control of the film stress of Cat-CVD a-Si films and its impact on explosive crystallization induced by flash lamp annealing
Author(s)	Ohdaira, Keisuke
Citation	Thin Solid Films, 575: 21-24
Issue Date	2015-01-30
Type	Journal Article
Text version	author
URL	http://hdl.handle.net/10119/13834
Rights	Copyright (C)2014, Elsevier. Licensed under the Creative Commons Attribution-NonCommercial-NoDerivatives 4.0 International license (CC BY-NC-ND 4.0). [http://creativecommons.org/licenses/by-nc-nd/4.0/] NOTICE: This is the author's version of a work accepted for publication by Elsevier. Keisuke Ohdaira, Thin Solid Films, 575, 2014, 21-24, http://dx.doi.org/10.1016/j.tsf.2014.10.018
Description	

The control of the film stress of Cat-CVD a-Si films and its impact on explosive crystallization induced by flash lamp annealing

Keisuke Ohdaira^{1,2}

¹Japan Advanced Institute of Science and Technology (JAIST)

1-1 Asahidai, Nomi, Ishikawa 923-1292, Japan

²PRESTO, Japan Science and Technology Agency (JST)

4-1-8 Honcho Kawaguchi, Saitama 332-0012, Japan

Phone: +81-3-761-51-1551 E-mail: ohdaira@jaist.ac.jp

Catalytic chemical vapor deposition (Cat-CVD) can produce amorphous silicon (a-Si) films with low film stress, in general, compared to plasma-enhanced CVD, and is thus suited for the preparation of precursor a-Si films for thick poly-Si films applied for solar cells. The stress of a-Si films is known to sometimes play an important role for the crystallization of a-Si films and resulting grain size of polycrystalline Si (poly-Si) films formed. I investigate the impact of the stress of Cat-CVD a-Si films on the mechanism of explosive crystallization (EC) induced by flash lamp annealing (FLA). The stress of Cat-CVD a-Si films can be controlled by changing the temperatures of substrates and/or a catalyzing wire during film deposition. Cat-CVD a-Si films with tensile stress (~200 MPa) can be deposited as well as films with compressive stress. The enlargement of grain size is observed in a part of flash-lamp-crystallized (FLC) poly-Si films formed from Cat-CVD films with tensile stress compared to those with

compressive stress, which might be an indication of a certain degree of impact of film stress on poly-Si formation. The grain size is, however, much smaller than that of FLC poly-Si films formed from electron-beam- (EB-) evaporated a-Si films with similar tensile stress. This fact may indicate the existence of other critical determinant of EC mechanism.

Keywords: flash lamp annealing, amorphous silicon, polycrystalline silicon, crystallization, film stress, explosive crystallization

1. Introduction

Thin-film polycrystalline silicon (poly-Si) solar cells have attracted a considerable interest because of its advantages such as long-term stability, low Si material usage, and low cost. A variety of methods have been investigated to obtain thin poly-Si [1-5], and the crystallization of precursor amorphous Si (a-Si) films by post-annealing is one of the most successful approaches to form poly-Si films [1-3]. We have so far investigated the utilization of flash lamp annealing (FLA), millisecond-order discharge from Xe lamps, to crystallize precursor a-Si films prepared on glass substrates [6-12]. Due to its proper annealing duration, FLA can form more than 4 μm -thick poly-Si films without serious thermal damage onto entire glass substrates [6,7]. The formation of such thick poly-Si films is also owing to the successful preparation of thick precursor a-Si films without peeling during their deposition by catalytic chemical vapor deposition (Cat-CVD). Cat-CVD can yield a-Si films with lower film stress than conventional plasma-enhanced CVD (PECVD). We have also revealed that the crystallization of a-Si films induced by FLA is based on explosive crystallization (EC), self-catalytic lateral crystallization driven by the release of latent heat [8-12]. To date, we have observed at least two modes of EC: 1) EC forming poly-Si films with periodic microstructures along a lateral crystallization direction containing solid-phase-nucleated (SPN) 10-nm-sized fine grains, and 2) EC based on liquid-phase epitaxy (LPE) which results in the formation of poly-Si films consisting only of large grains with a length of $>10 \mu\text{m}$ stretching along an EC direction. The former is observed when Cat-CVD and sputtered a-Si films are used, while the latter appears if we use electron-beam- (EB-) evaporated a-Si films as precursor films [10]. One possible reason for the emergence of different EC modes is the effect of the stress of a-Si films which could affect the

probability of SPN [13]. Cat-CVD and sputtered a-Si films which we used previously have compressive stress, while EB-evaporated a-Si films have tensile stress, and SPN in EB-evaporated a-Si films with tensile stress might be suppressed. In order to clarify the impact of the stress of precursor a-Si films on EC modes, I have attempted to prepare Cat-CVD a-Si films with tensile stress by tuning deposition parameters, and performed FLA onto the a-Si films with tensile stress. I have confirmed that a-Si films with a tensile stress of more than 200 MPa can be formed by Cat-CVD by increasing catalyzer temperature (T_{cat}) and decreasing substrate temperature (T_{sub}).

2. Experimental procedures

I performed the deposition of a-Si films by Cat-CVD under the conditions summarized in Table I. Substrate holder temperature (T_{holder}) and T_{cat} were changed systematically, whereas other parameters were fixed. A T_{cat} of 1750 °C and a T_{holder} of 450 °C are the conditions which we have used previously to prepare precursor a-Si films [6-8, 10]. It should be noted that I only measured T_{holder} , using a thermocouple connected to the holder, which is not equal to an actual T_{sub} . The deposition rate of a-Si films was ~100 nm/min, which was almost independent of T_{cat} and T_{holder} . I used crystalline Si (c-Si) substrates with a size of 50×7×0.2 mm³ for the measurement of the stress of a-Si films. About 1-μm-thick a-Si films were deposited on the Si substrates, and their warping was measured on a stylus profiler. The following Stoney formula was applied to evaluate film stress [14]

$$\sigma = \frac{E_s d_s^2}{6(1-\nu_s) R d_f}, \quad (1)$$

Where σ , E_s , d_s , ν_s , R , and d_f represent film stress, Young's modulus of c-Si, the thickness of a c-Si substrate, Poisson's ratio of c-Si, radius of curvature, and the thickness of an a-Si film, respectively. The warping of the Si wafers before a-Si deposition was negligibly small. Cat-CVD a-Si films deposited on high-resistivity ($>1000 \text{ } \Omega\text{cm}$) Si wafers were also characterized by Fourier-transform infrared (FT-IR) spectroscopy.

For the formation of flash-lamp-crystallized (FLC) poly-Si films, I first deposited 200-nm-thick Cr films on $20 \times 20 \times 0.7 \text{ mm}^3$ -sized Eagle XG glass substrates as adhesion layers [15]. Cat-CVD a-Si films with a thickness of $4.5 \text{ } \mu\text{m}$ were then deposited onto the Cr-coated glass substrates. FLA was performed at a fluence of $\sim 15 \text{ J/cm}^2$ with a duration of $\sim 7 \text{ ms}$ under Ar atmosphere with supporting holder heating at $400 \text{ } ^\circ\text{C}$. Only one shot of flash lamp light was supplied for each sample, and no dehydrogenation process prior to FLA was performed. The details of our FLA system have been summarized elsewhere [10]. FLC poly-Si films were characterized by optical microscopy and Raman spectroscopy. The 632.8 nm line of a He-Ne laser was used for the Raman measurement.

3. Results and discussion

Figure 1 shows the stress of Cat-CVD a-Si films as a function of T_{holder} at a fixed T_{cat} of $1750 \text{ } ^\circ\text{C}$. The a-Si films which we have used previously have a compressive stress of 350 MPa . The compressive stress of a-Si films decreases monotonically with decrease in T_{holder} , and the stress becomes close to 0 at a T_{holder} of $50 \text{ } ^\circ\text{C}$. Reduction in T_{sub} generally leads to the formation of a-Si films with less density, due to less active migration of radicals on the film surface, which can be a cause of the decreased

compressive stress. Figure 2 shows the FT-IR spectra of Cat-CVD a-Si films deposited at T_{holder} of 50-450 °C around 2000 cm^{-1} , indicating stretching modes of Si-H and Si-H₂ bonds. The intensity of the Si-H₂ peaks tends to increase as T_{holder} decreases. This fact indicates that less dense a-Si films are formed at lower T_{holder} , and is consistent with the tendency of the stress variation. The tendency of lower compressive stress at lower T_{sub} is also seen in PECVD a-Si films [16,17].

Figure 3 shows the stress of Cat-CVD a-Si films as a function of T_{cat} at T_{holder} of 50 and 450 °C. The film stress turns from compressive to tensile and the value of tensile stress increases with increase in T_{cat} for both T_{holder} . It should be emphasized that Cat-CVD a-Si films with a tensile stress of more than 200 MPa are formed at a T_{cat} of ~2000 °C. The tendency of more tensile stress at higher T_{cat} cannot be described by film density, since T_{sub} is probably higher at higher T_{cat} due to radiation from the W catalyzer, and I do not observe any increase in the ratio of SiH₂/SiH stretching mode peak intensity with increase in T_{cat} in the FT-IR spectra of the deposited a-Si films. Figure 4 shows H content in the Cat-CVD a-Si films, evaluated from the Si-H wagging mode peak of FT-IR spectra, as a function of T_{cat} . One can see clear tendency of lower H content at higher T_{cat} . PECVD hydrogenated a-Si films tend to have less compressive stress if they contain less H atoms [18], and similar phenomenon is probably observed in the Cat-CVD a-Si films studied here. The reason of lower H content at higher T_{cat} may be because of the more active extraction of H atoms from deposited films during deposition by larger amount of radicals generated due to more enhanced decomposition of gas molecules on the W catalyzer. This effect might be related to the less effect of T_{holder} on film stress at higher T_{cat} shown in Fig. 3. The amount of H atoms in Cat-CVD a-Si films probably has no significant impact on the

mechanism of EC, since EC leaving behind periodic structures occurs also in sputtered a-Si films containing little H atoms [9]. It should be noted that the formation of Cat-CVD a-Si films with similar tensile stress has also been reported by Mahan [19], which is realized by systematically changing H₂ flow rate.

Figure 5 shows the surface microscopic images of FLC poly-Si films formed from Cat-CVD a-Si films with tensile and compressive stress. Typical periodic structure is seen on the surface of a FLC film formed from an a-Si film with compressive stress (Fig. 5(c)). This characteristic periodic structure results from the alternative emergence of SPN-dominant and LPE-involved crystallizations [8], and the lateral crystallization speed of this particular EC mode has been estimated to be 4 m/s [10]. Similar periodic structure is also seen on part of the surface of a FLC poly-Si film formed from a Cat-CVD a-Si film with tensile stress (Fig. 5(a)), meaning that EC occurs under the same mechanism in this region. On the other hand, such a characteristic surface morphology is not seen on some parts of the surface of the same FLC poly-Si film (Fig. 5(b)), and rather more like the surface of a FLC poly-Si film formed from an EB-evaporated a-Si film (Fig. 5(d)). This might be an indication of the partial emergence of other type of EC.

Figure 6 shows the Raman spectra of FLC poly-Si films formed from Cat-CVD a-Si films with tensile and compressive stress, the measurement positions of which corresponds to Figs. 5(a)-(c). The c-Si Raman peak of the poly-Si film formed from an a-Si film with compressive stress locates at 520.5 cm⁻¹, almost equal to that of a c-Si wafer. This means that the original compressive stress of the Si film is relaxed during crystallization. As has been mentioned previously, the EC leaving behind periodic microstructures is based on the alternative emergence of SPN-dominant and

LPE-involved crystallization, and the formation of protrusions in the LPE-involved regions may be one of possible explanations for the stress relaxation. The spectra of FLC poly-Si films formed from Cat-CVD a-Si films with tensile stress have c-Si peaks at lower Raman shift. This indicates that original tensile stress is remained even in the FLC poly-Si films. One can also see that the c-Si peak of the Raman spectrum observed from the flat surface region has smaller full-width at half maximum (FWHM) than that from rough surface region, which is an indication of the formation of larger grains [20].

The peak position and FWHM of c-Si Raman peaks are summarized in Table II. The positions of c-Si Raman peaks of FLC poly-Si films formed from a-Si films with tensile stress are almost equal to that formed from EB-evaporated a-Si films, while there is large difference in their FWHM, 6.0 cm^{-1} and 4.5 cm^{-1} . This fact means that the size of grains in FLC poly-Si films formed from a-Si films with tensile stress is significantly smaller than that in FLC poly-Si films formed from EB-evaporated a-Si films. It is thus considered that a limiting factor other than the stress of precursor a-Si films may also exist, although there may be a certain degree of an impact of film stress on EC mechanism.

4. Conclusion

The stress of Cat-CVD a-Si films can be widely controlled by changing T_{sub} and/or T_{cat} , and a-Si films with tensile stress ($\sim 200 \text{ MPa}$) as well as compressive stress can be produced. Decrease in T_{sub} and/or increase in T_{cat} lead to the formation of less compressive (more tensile) a-Si films. FLC poly-Si films formed from a-Si films with

tensile stress still consist of much finer grains than that formed from EB-evaporated a-Si films. Thus, there may also be other critical determinant of the EC mechanism.

Acknowledgment

The author would like to thank L. Yang of JAIST for her assistance of FLA and Cat-CVD experiments. This work was supported by JST PRESTO program.

References

- [1] T. Matsuyama, M. Tanaka, S. Tsuda, S. Nakano, Y. Kuwano, *Jpn. J. Appl. Phys.* 32 (1993) 3720.
- [2] M.J. Keevers, T.L. Young, U. Schubert, M.A. Green, 22nd European Photovoltaic Solar Energy Conference, Milan, Italy, September 3–7, 2007, p. 1783, and references therein.
- [3] I. Gordon, D. Van Gestel, L. Carnel, G. Beaucarne, J. Poortmans, K.Y. Lee, P. Dogan, B. Gorka, C. Becker, F. Fenske, B. Rau, S. Gall, B. Rech, J. Plentz, F. Falk, D. Le Bellac, Proceedings of the 22nd European Photovoltaic Solar Energy Conference, Milan, Italy, September 3–7, 2007, p. 1890, and references therein.
- [4] S. Janz, M. Kuenle, S. Lindekugel, E.J. Mitchell, S. Reber, Proceedings of the 33 rd IEEE Photovoltaic Specialists Conference, San Diego, U.S.A., May 11–16, 2008, p. 1805, and references therein.
- [5] K.Y. Lee, C. Becker, M. Muske, F. Ruske, S. Gall, B. Rech, M. Berginski, J. Hüpkes, *Appl. Phys. Lett.* 91 (2007) 241911.
- [6] K. Ohdaira, Y. Endo, T. Fujiwara, S. Nishizaki, H. Matsumura, *Jpn. J. Appl. Phys.* 46 (2007) 7603.
- [7] K. Ohdaira, T. Fujiwara, Y. Endo, S. Nishizaki, H. Matsumura, *Jpn. J. Appl. Phys.* 47 (2008) 8239.
- [8] K. Ohdaira, T. Fujiwara, Y. Endo, S. Nishizaki, H. Matsumura, *J. Appl. Phys.* 106 (2009) 044907.
- [9] K. Ohdaira, S. Ishii, N. Tomura, H. Matsumura, *J. Nanosci. Nanotech.* 12 (2012) 591.

- [10] K. Ohdaira, N. Tomura, S. Ishii, H. Matsumura, *Electrochem. Solid-State Lett.* 14 (2011) H372.
- [11] K. Ohdaira, H. Matsumura, *J. Cryst. Growth* (in press).
- [12] K. Ohdaira, K. Sawada, N. Usami, S. Varlamov, H. Matsumura, *Jpn. J. Appl. Phys.* (in press).
- [13] H. Fujiwara, M. Kondo, A. Matsuda, *Jpn. J. Appl. Phys.* 41 (2002) 2821.
- [14] G. G. Stoney, *Proc. R. Soc. A* 82 (1909) 172.
- [15] K. Ohdaira, T. Fujiwara, Y. Endo, K. Shiba, H. Takemoto, H. Matsumura, *Jpn. J. Appl. Phys.* 49 (2010) 04DP04.
- [16] S. Nonomura, N. Yoshida, T. Gotoh, T. Sakamoto, M. Kondo, A. Matsuda, S. Nitta, *J. Non-Cryst. Solids* 266 (2000) 474.
- [17] K. S. Stevens, N. M. Johnson, *J. Appl. Phys.* 71 (1992) 2628.
- [18] Y. Q. Fu, J. K. Luo, S. B. Milne, A. J. Flewitt, W. I. Milne, *Mater. Sci. Eng. B* 124 (2005) 132.
- [19] A. H. Mahan, *Thin Solid Films* 501 (2006) 3.
- [20] C. Smit, R. A. C. M. M. van Swaaij, H. Donker, A. M. H. N. Petit, W. M. M. Kessels, M. C. M. van de Sanden, *J. Appl. Phys.* 94 (2003) 3582.

Table and figure captions

Table I Deposition conditions of a-Si films by Cat-CVD.

Table II Comparison of the position and FWHM of c-Si Raman peaks of FLC poly-Si films. The data of a c-Si wafer is also shown for comparison.

Fig. 1 Stress of Cat-CVD a-Si films as a function of T_{holder} at a fixed T_{cat} of 1750 °C.

Fig. 2 FT-IR spectra of Cat-CVD a-Si films deposited at various T_{holder} .

Fig. 3 Stress of Cat-CVD a-Si films as a function of T_{cat} at T_{holder} of 50 and 450 °C.

Fig. 4 H content in Cat-CVD a-Si films estimated from the area of Si-H wagging mode peaks as a function of T_{cat} .

Fig. 5 Surface images of FLC poly-Si films formed from (a)(b) a Cat-CVD a-Si film with tensile stress (~200 MPa), (c) a Cat-CVD a-Si film with compressive stress (~-350 MPa), and (d) an EB-evaporated a-Si film.

Fig. 6 Raman spectra of FLC poly-Si films formed from Cat-CVD a-Si films with tensile and compressive stress.

Table I K. Ohdaira,

SiH ₄ flow rate	50 sccm
H ₂ flow rate	10 sccm
Pressure	1.1 Pa
Substrate holder temperature	50-450 °C
W temperature	1700-2100 °C
Catalyzer-substrate distance	12 cm
W wire length	260 cm
Chamber volume	~100,000 cm ³

Table II K. Ohdaira,

	Peak position	FWHM
Tensile (rough)	517.5 cm ⁻¹	7 cm ⁻¹
Tensile (flat)	517.5 cm ⁻¹	6 cm ⁻¹
Compressive	520.5 cm ⁻¹	7 cm ⁻¹
EB evaporation	517.5 cm ⁻¹	4.5 cm ⁻¹
Si wafer	520.5 cm ⁻¹	4 cm ⁻¹

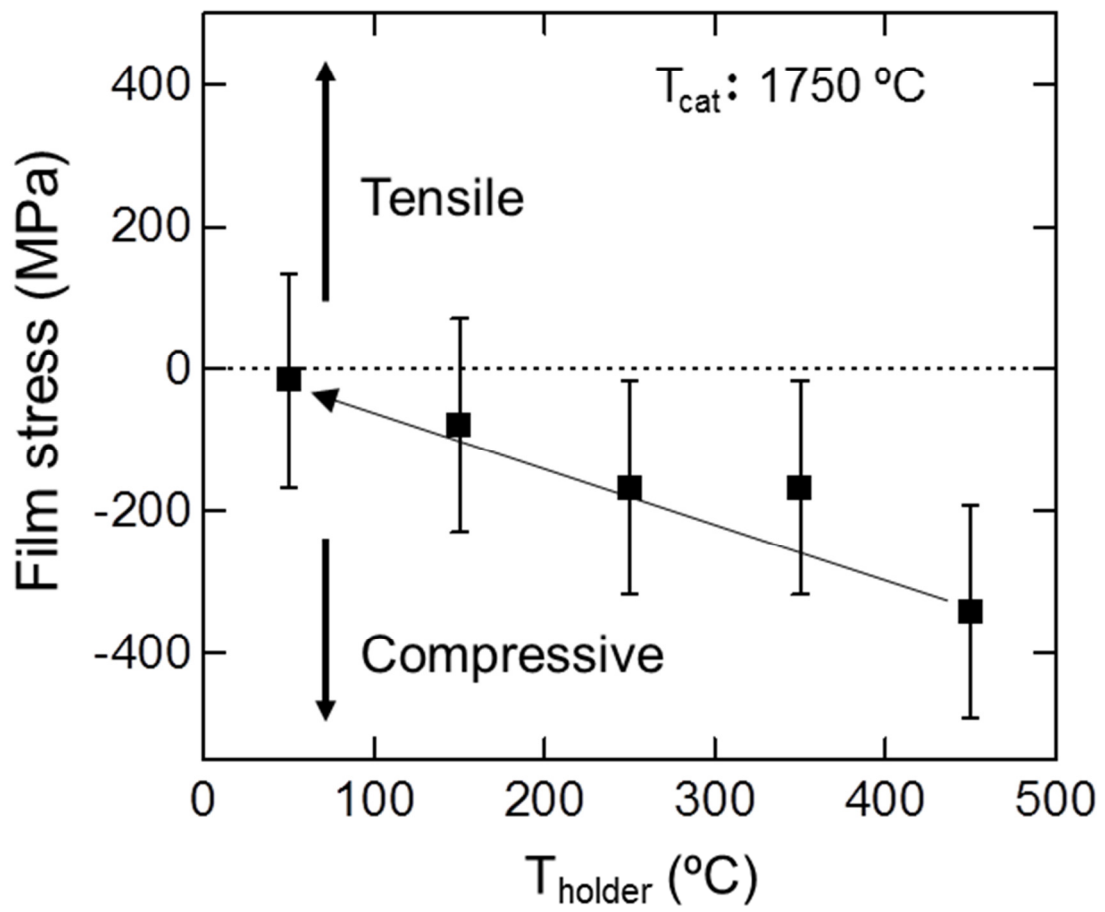


Figure 1 K. Ohdaira,

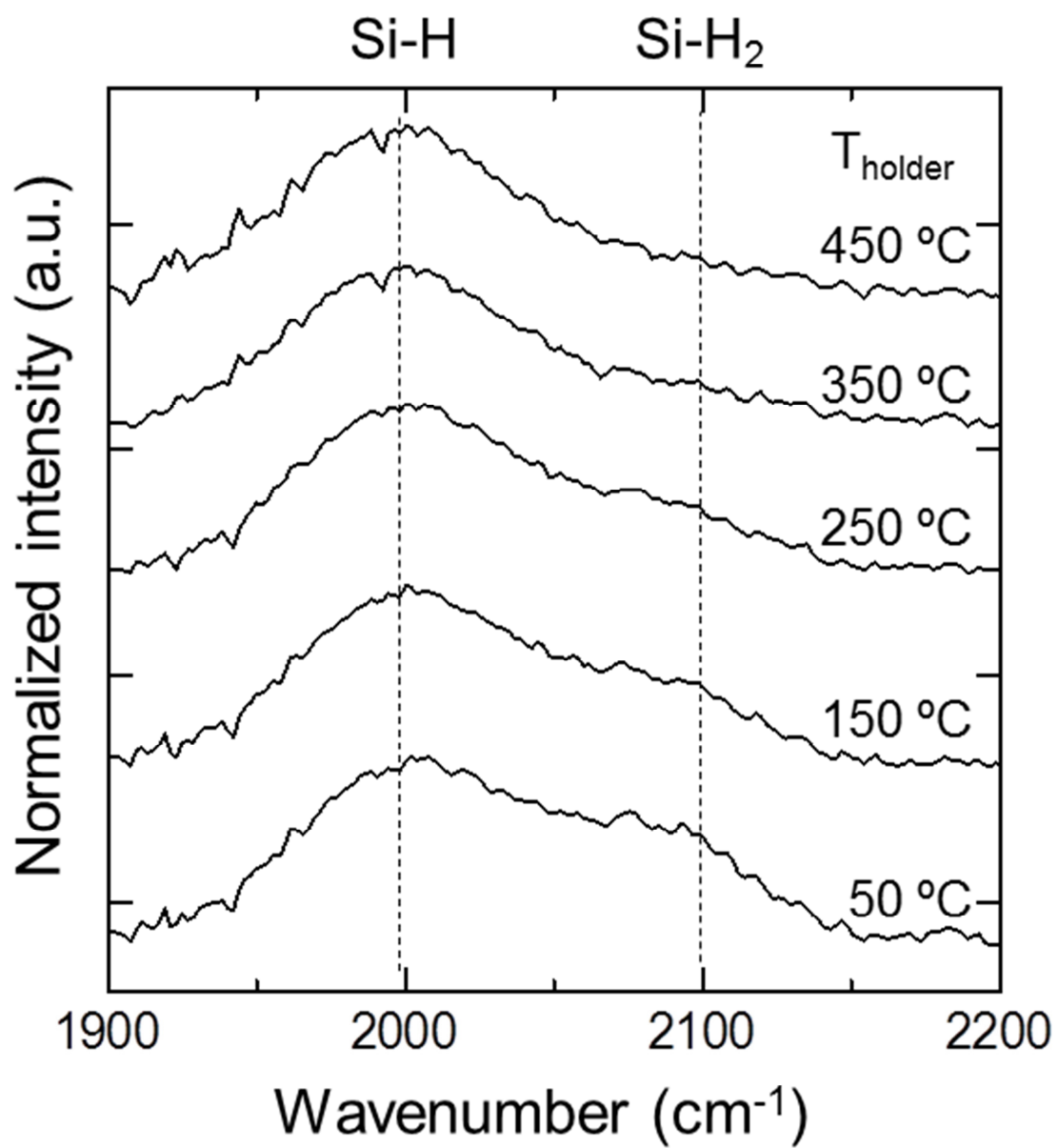


Figure 2 K. Ohdaira,

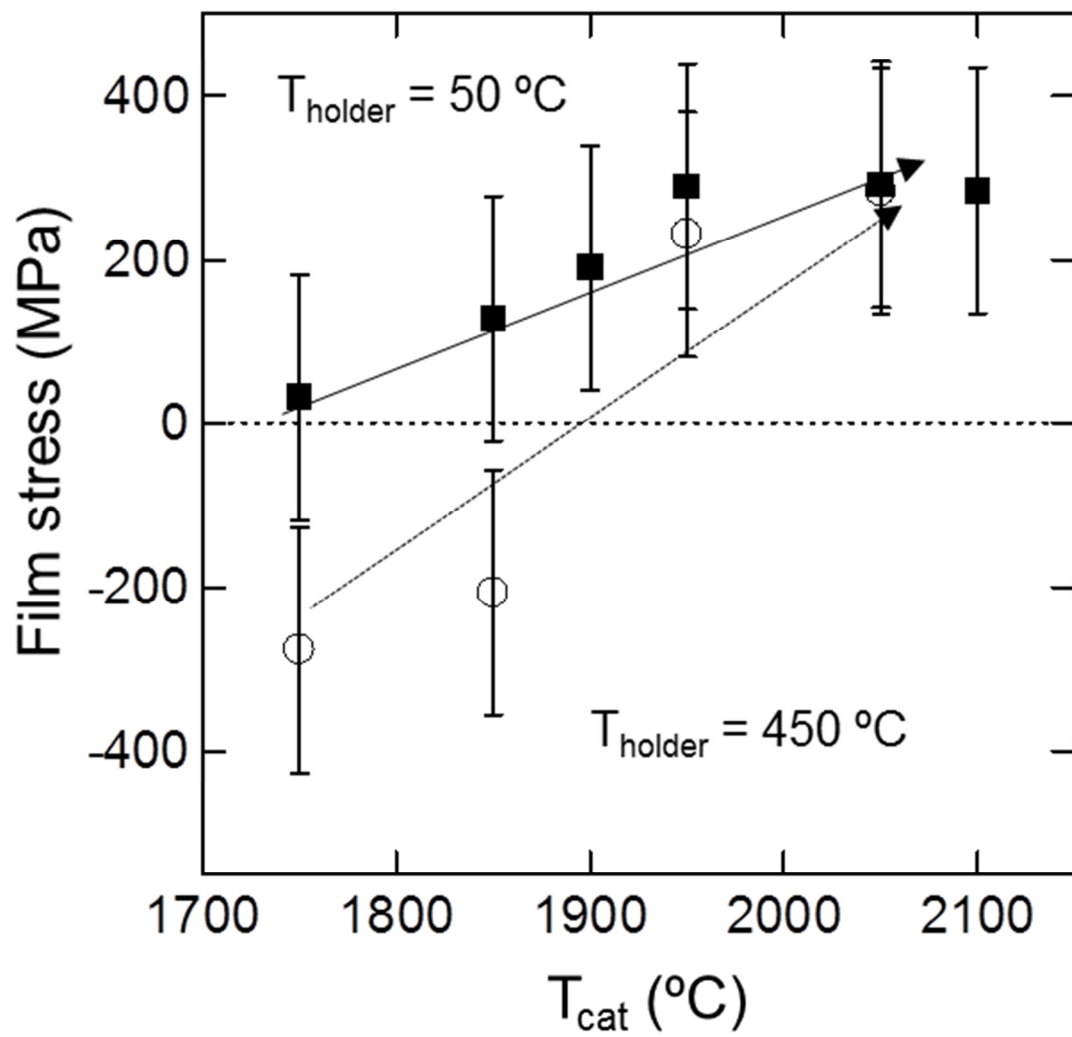


Figure 3 K. Ohdaira,

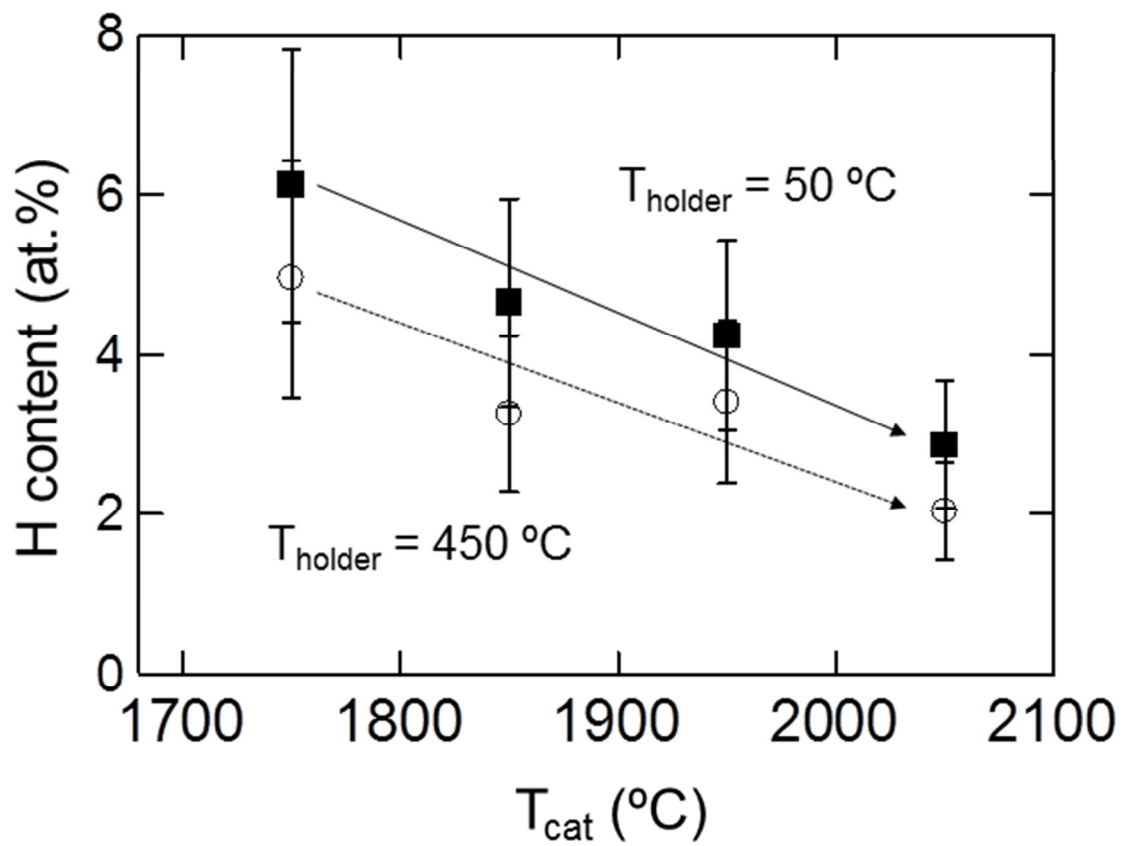


Figure 4 K. Ohdaira,

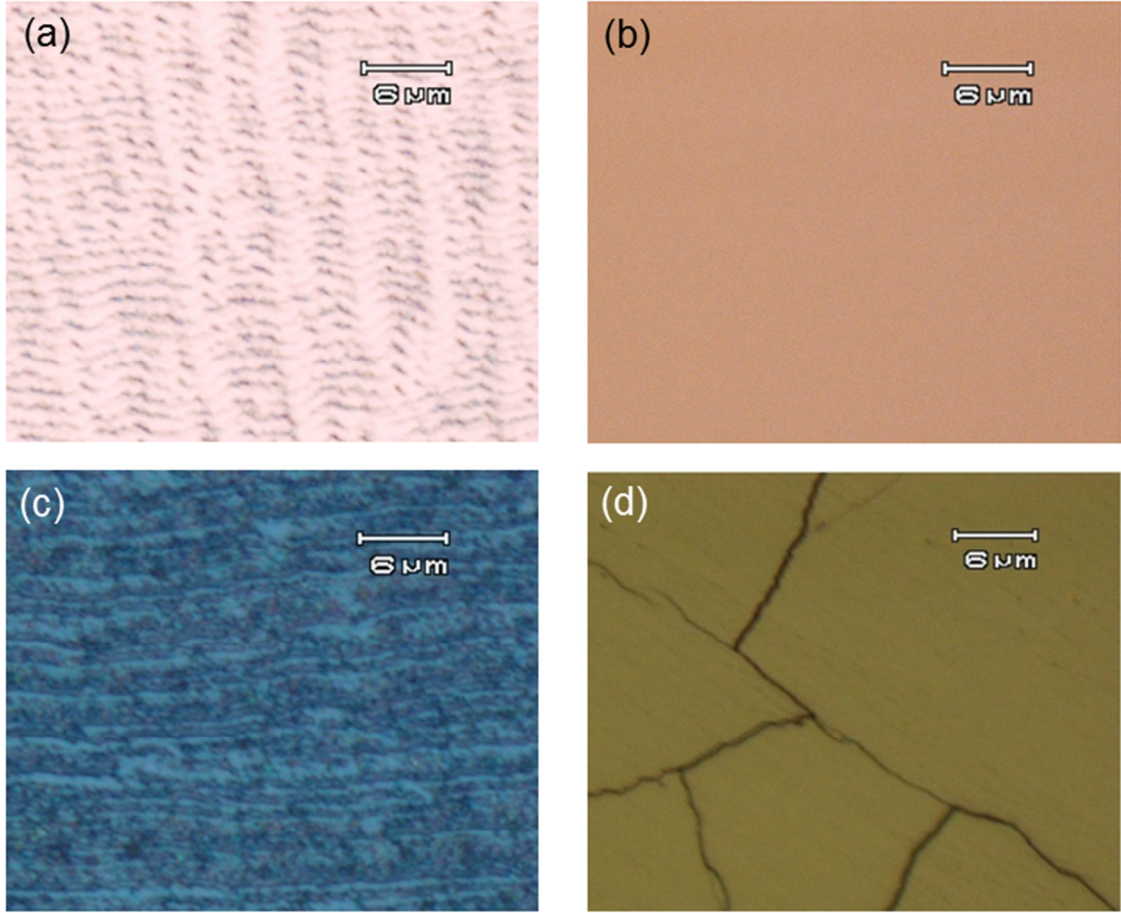


Figure 5 K. Ohdaira,

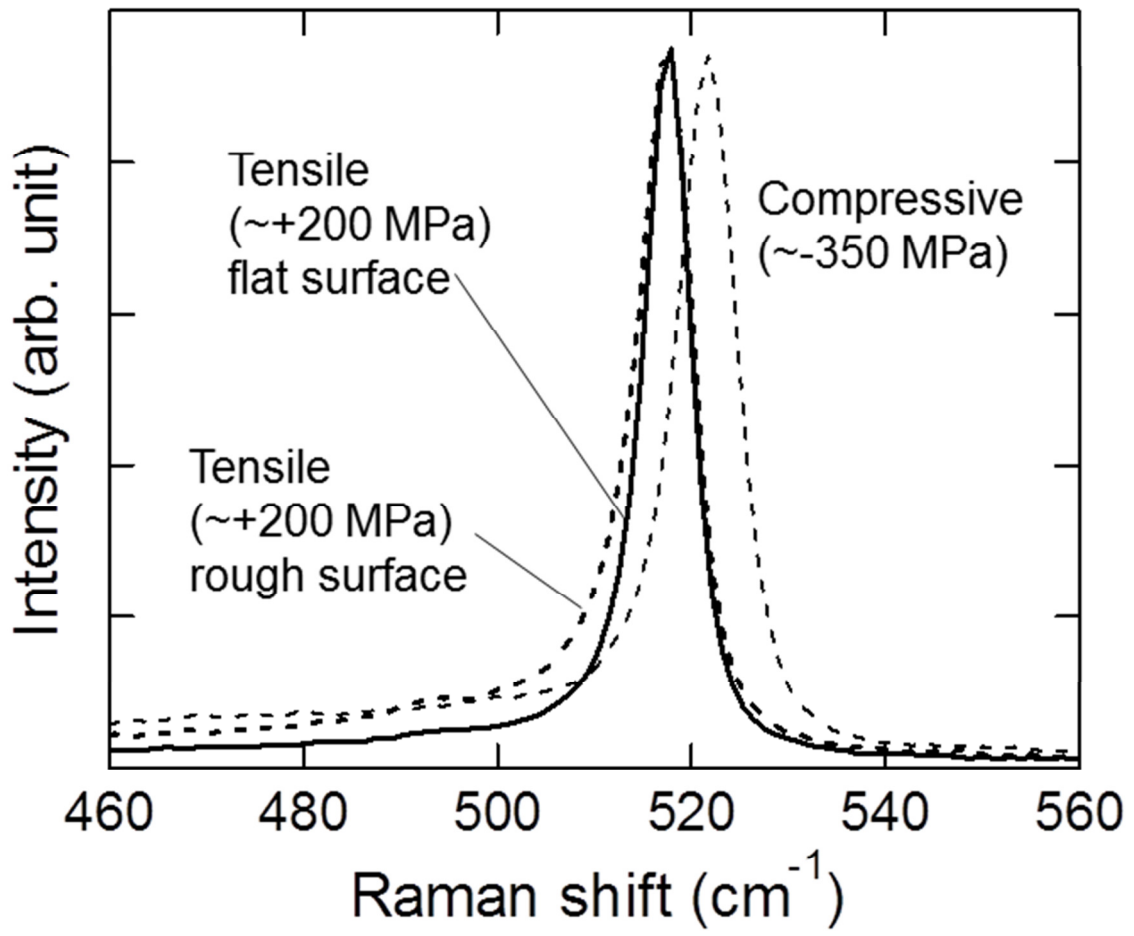


Figure 6 K. Ohdaira,